Recent results from fixed-target collisions at LHCb

Kara Mattioli[1]*, on behalf of the LHCb collaboration

[1]Laboratoire Leprince Ringuet, École polytechnique, 91128 Palaiseau, France

Abstract. The LHCb spectrometer has the unique capability to function as a fixed-target experiment by injecting gas into the LHC beam pipe while proton or ion beams are circulating. The resulting beam+gas collisions have a center of mass energy intermediate to previous fixed-target experiments and the top RHIC energy for AA collisions, cover an unexplored kinematic range and allow systems of different size to be studied. Here we present new results on open charm, J/ψ, and $\psi(2S)$ production from pNe and PbNe fixed-target collisions at LHCb. Comparisons with various theoretical models of particle production and transport through the nucleus will be discussed.

1 The fixed-target program at LHCb

The LHCb detector at the LHC is a fully-instrumented single-arm spectrometer covering the forward pseudorapidity region between $2 < \eta < 5$ [1]. Thanks to its System for Measuring Overlap with Gas (SMOG), the LHCb detector can operate as both a collider and fixed-target experiment [2]. During the LHC Run 2, SMOG was used to inject small amounts of noble gases into the LHC beam pipe near the LHCb interaction point and one of the circulating LHC beams was used to create proton-gas and Pb-gas collisions. The resulting fixed-target collisions in LHCb provide access to rapidity in the center of mass system y^* between -2.29 and 0 and cover a larger Bjorken x ($\sim 10^{-1}$) and lower Q^2 phase space than that probed in collider-mode collisions [2]. Recent measurements of charmonium and D^0 production in pNe and PbNe collisions were performed using fixed-target datasets collected by LHCb in 2017 and 2018, respectively [3]-[5]. Both datasets were collected using a 2.5 TeV beam from the LHC incident on Neon gas atoms, resulting in a nucleon-nucleon center of mass energy $\sqrt{s_{NN}}$ of 68.5 GeV. These measurements are compared to various theoretical models and are also used to study cold nuclear matter effects on hidden and open charm mesons.

2 Charm production in *p*Ne and PbNe collisions

Measurements of hidden and open charm meson production in pNe collisions were performed with the 2017 dataset, which corresponds to an integrated luminosity of $\mathcal{L} = 21.7 \pm 1.4$ nb^{-1}. D^0 meson candidates were reconstructed in the decay channel $D^0 \to K^-\pi^+$, while the J/ψ and $\psi(2S)$ candidates were reconstructed in the dimuon decay channel [3, 4]. All three charm hadrons were selected with $p_T < 8$ GeV/c and rapidity in the laboratory frame $2.0 < y < 4.29$. The differential cross sections per nucleon for D^0 meson production, computed by dividing the measured cross section by the number of nucleons in Neon (20.1798 accounting for the

*e-mail: kara.mattioli@llr.in2p3.fr

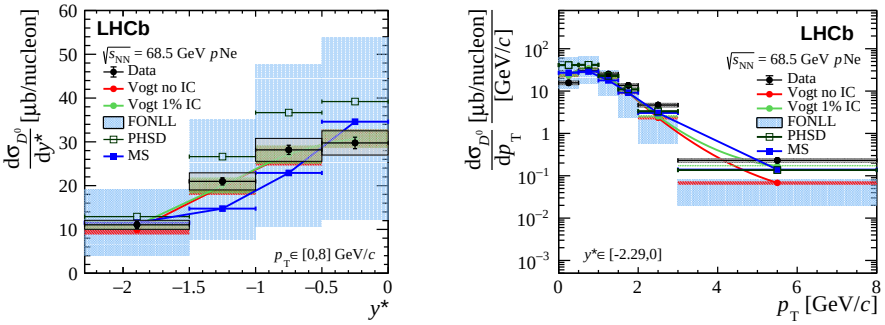

Figure 1: The differential cross sections for D^0 production in pNe collisions as a function of the D^0 (left) y^* and (right) p_T [3]. The LHCb data points in black are compared to a variety of theoretical models (see text for details).

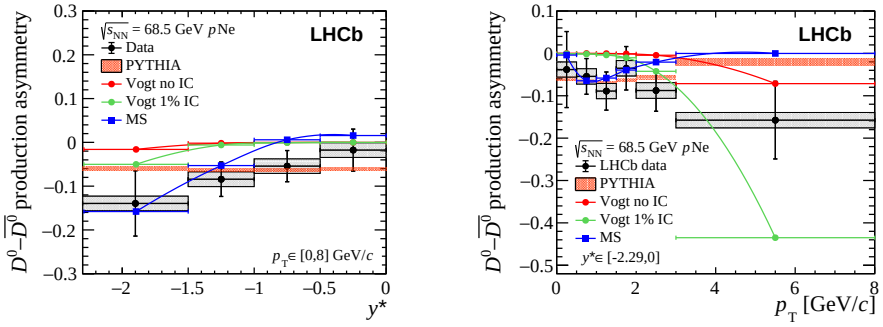

Figure 2: The $D^0 - \overline{D^0}$ production asymmetry in pNe collisions as a function of the D^0 (left) y^* and (right) p_T. [3]

isotope), were measured as a function of the D^0 y^* and p_T and are shown in Figure 1. The LHCb measurements, shown in the black data points, are compared to theoretical models that take into account a variety of cold nuclear matter effects. The predictions from Vogt include nuclear shadowing effects and are shown with and without a 1% intrinsic charm (IC) contribution included [6]. The MS predictions include a 1% IC contribution and 10% recombination contributions [7]. The parton-hadron-string dynamics (PHSD) prediction [8] is a transport model calculation, and the FONLL predictions [9, 10] are a fixed-order plus next-to-leading-logarithms calculation with uncertainties from the factorization scale and parton distribution functions included. The $D^0 - \overline{D^0}$ production asymmetry, which probes charm quark hadronization with a high-x valence quark, was also measured as a function of the D^0 y^* and p_T and is shown in Figure 2. The results are compared to several of the same theoretical models as described above, as well as to PYTHIA [11].

The production of hidden charm mesons was also studied in pNe collisions [4]. Figure 3 shows the measured differential cross sections for J/ψ production as a function of the J/ψ y^* and p_T. The LHCb data points are compared to Leading-Order Color Singlet Model (LO CSM) predictions computed using the HELAC-Onia generator and to predictions by Vogt [6] that were computed with the Color Evaporation Model and include contributions from nuclear absorption of the $c\bar{c}$ state and multiple scattering. The L0 CSM predictions do not describe the

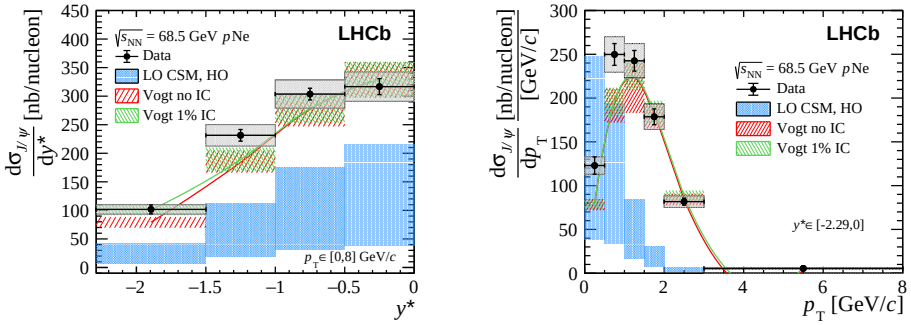

Figure 3: The differential cross sections for J/ψ production in pNe collisions as a function of the J/ψ (left) y^* and (right) p_T [4]. The LHCb data points in black are compared to several theoretical models (see text for details).

trends observed in data, indicating the need for higher-order calculations to describe the J/ψ production. The Vogt predictions describe both of the observed y^* and p_T trends, however the current precision in the data cannot yet distinguish between predictions with or without a 1% IC component. The J/ψ total cross section per target nucleon was also measured and found to be consistent with the trend established by previous measurements of the total J/ψ cross section as a function of $\sqrt{s_{NN}}$ [4]. Due to the limited sample size, similar cross section measurements were not made for the $\psi(2S)$ and instead the relative production rate of $\psi(2S)$ and J/ψ mesons was measured and found to be in good agreement with measurements on other nuclear targets and at similar center of mass energies [4].

D^0 and J/ψ production were also measured in PbNe collisions to compare open and hidden charm production between large and small nuclear systems [5]. The J/ψ to D^0 cross section ratio was measured in PbNe collisions and compared to the same ratio measured in pNe collisions. The ratio in collisions of nuclei with mass numbers A and B is assumed to have the functional form $\sigma^{AB}_{J/\psi}/\sigma^{AB}_{D^0} = \sigma^{pp}_{J/\psi}/\sigma^{pp}_{D^0} \times (N_{coll})^{\alpha-1}$, where N_{coll} is the number of binary nucleon-nucleon collisions obtained from a Glauber analysis [5]. An α value less than one indicates that J/ψ mesons experience additional nuclear effects than D^0 mesons. The cross section ratio as a function of N_{coll} is shown in the left image of Figure 4. The fitted α value smaller than one indicates that the J/ψ mesons do experience more nuclear effects in PbNe collisions than D^0 mesons. Within the current experimental uncertainties, a linear trend is observed between pNe collisions and central PbNe collisions, preventing the conclusive observation of anomalous J/ψ suppression or the formation of a deconfined medium. Future measurements with LHCb's upgraded fixed-target gas injection cell for Run 3, SMOG2, will have much smaller statistical and systematic uncertainties to enable more precise measurements of charmonia production [12]. The right image of Figure 4 shows the excellent J/ψ yield collected in 18 minutes of pAr data-taking during SMOG2 commissioning [13].

3 Conclusion

Measurements of D^0 and charmonium production have recently been performed in $\sqrt{s_{NN}}$ = 68.5 GeV pNe and PbNe collisions with the LHCb detector in its fixed-target configuration. In pNe collisions, the $D^0 - \overline{D^0}$ production asymmetry and differential D^0 and J/ψ cross sections as a function of the hadron y^* and p_T were measured and compared with theoretical calculations incorporating a variety of cold nuclear matter effects. The first fixed-target AA

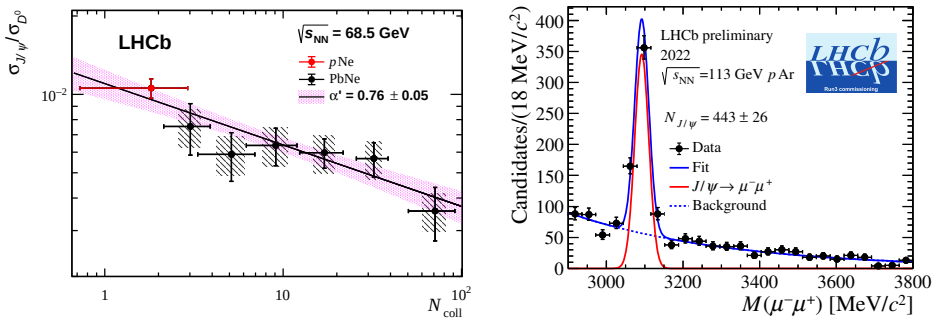

Figure 4: (left) The J/ψ to D^0 cross section ratio as a function of the number of binary nucleon-nucleon collisions N_{coll} [5] (right) the J/ψ yield in pAr collisions using the upgraded SMOG2 system [13]

experiment at the LHC was performed with PbNe collisions, and no anomalous J/ψ suppression is observed within the current experimental uncertainties. LHCb's upgraded fixed-target system, SMOG2, is now operational in Run 3 and will collect much larger samples of fixed-target collisions with a variety of nuclear targets, enabling detailed studies of charm production in a variety of nuclear systems.

References

[1] The LHCb Collaboration, *The LHCb detector at the LHC*, JINST **3**, S08005 (2008).

[2] A. Bursche *et. al. Physics opportunities with the fixed-target program of the LHCb experiment using an unpolarized gas target*, LHCb-PUB-2018-015.

[3] The LHCb Collaboration, *Open charm production and asymmetry in pNe collisions at* $\sqrt{s_{NN}}$ *= 68.5 GeV*, EPJC **83**, 541 (2023).

[4] The LHCb Collaboration, *Charmonium production in pNe collisions at* $\sqrt{s_{NN}}$ *= 68.5 GeV*, EPJC **83**, 625 (2023).

[5] The LHCb Collaboration, *J/ψ and* D^0 *production in* $\sqrt{s_{NN}}$ *= 68.5 GeV PbNe collisions*, EPJC **83**, 658 (2023).

[6] R. Vogt, *Limits on intrinsic charm production from the SeaQuest experiment*, Phys. Rev. **C103**, 035204 (2021).

[7] R. Maciula and A. Szczurek, *Recombination mechanism for* D^0*-meson production and* $D^0 - \overline{D^0}$ *production asymmetry in the LHCb* p+^{20}*Ne fixed-target experiment*, Phys. Lett. **B835**, 137530 (2022).

[8] T. Song *et al.*, *Single electrons from heavy-flavor mesons in relativistic heavy-ion collisions* Phys. Rev. **C96**, 014905 (2017).

[9] M. Cacciari, P. Nason, and R. Vogt, *QCD predictions for charm and bottom quark production at RHIC*, Phys. Rev. Lett. **95**, 122001 (2005).

[10] M. Cacciari, M. Greco, and P. Nason, *The* p_T *spectrum in heavy-flavour hadroproduction*, JHEP **05**, 007 (1998).

[11] T. Sjöstrand, S. Mrenna, and P. Skands, *A brief introduction to* Pythia 8.1 Comput. Phys. Commun. **178**, 852 (2008).

[12] The LHCb Collaboration, *LHCb SMOG Upgrade*, LHCb-TDR-020.

[13] The LHCb Collaboration, LHCb-FIGURE-2023-008.